

iCushion: A Pressure Map Algorithm for High Accuracy Human Identification

^{1,2,3}Haojun Ai

⁴Liezhao Zhang

⁴Zhiyu Yuan

⁴Haitao Huang

¹ Key Laboratory of Aerospace Information Security and Trusted Computing, Ministry of Education, China

² School of Cyber Science and Engineering, Wuhan University, China

³ Collaborative Innovation Center of Geospatial Technology

⁴ Computer School, Wuhan University, China

aihj@whu.edu.cn

Abstract—Intelligent Cushion (iCushion) technology is recently booming with embedded pressure array sensors to enable individual-specific sitting experiences. iCushion has the build-in functionality to identify users throughout its use in a continuous and non-intrusive manner. Due to the variability in sitting posture and the angle of seated deflection, the accuracy of user identification remains unstable or unclear with existing solutions. Aiming at this problem, this study develops a two-stage pressure map algorithm based on robust spatial-temporal features. First, pressure maps are collected constantly without limiting the user's posture, based on which an accumulated identity library is established for sitting postures by extracting features from pressure maps. To be specifically, we create a decision tree to classify maps by distances between both ischia and then variances in both areas around ischia in maps are analyzed. Second, the similarity between both maps are measured by the Euclidean distance between feature vectors around ischia for matching maps data. A k-NN voting mechanism is developed to achieve reliability of identification. The resulted iCushion prototype has successfully identified 92.2% of maps with three randomly chosen individuals through four-hour non-stop testing. It holds potentials of non-intrusive and reliable activity recognition in other pervasive applications.

Keywords—individual identification; pressure array sensors; continuous and non-intrusive

I. INTRODUCTION

In recent years, many researchers have attempted to extract large amounts of information which carry behavioral or individual characteristics from pressure data collected from various parts of the body to identify people or provide personalized services [1-3]. Pressure array sensors have become very popular for behavior analysis or identification of a variety of wearable and non-wearable devices. These sensors are easily embedded into cushions, mats, and other equipment commonly subject to daily use. Pressure array sensors can be used for behavioral analysis, such as the real-time recognition of patient intentions [4], recognizing and counting gym exercises [5], using sitting postures to control wheelchair

motion [6], and identifying individuals from their footsteps [7-9] or sitting postures [10-12].

Sitting is an entirely ubiquitous human behavior. People use sitting postures to work, drive, eat, and perform countless other activities throughout a given day. In this study, we tested a set of pressure array sensors to extract the inner features of sitting postures for human authentication. Compared to similar, previously published techniques, our approach allows for continuous and non-intrusive identification from a wide array of sitting postures – even deflected sitting postures – which is more user-friendly and with less demand for consistency in sitting postures.

A. Previous Studies

Marcello Ferro et al. employed MLP and KSOM classifiers to classify the 28-dimensional vectors collected by pressure array sensors with 28 pressure sensors in a particular sitting position; they achieved a high degree of correct classification in terms of acceptance and rejection rates.

Andreas Riener et al. calculated the Euclidean distance between feature vectors including “Pelvic Bones”, “Mid to High Pressure Area”, “High Pressure Area”, and “Weight” for different pressure maps to identify individuals.

M. Yamada et al. used a chair with pressure sensors attached to collect data from two stages, transient and stable, and classified them by SVM at a recognition accuracy over 90%.

The algorithms described above function using only a set of sitting postures provided a priori. In fact, however, any individual's sitting posture changes frequently throughout their life – indeed, throughout any given day – and thus creates significant differences in the resulting pressure maps. If a sitter uses a posture that is not in the sample dataset input to the pressure array sensors, there is no guarantee that he or she will be correctly identified. Additionally, the algorithms fail if the direction of the pressure maps are not parallel to the edge of the chair.

B. Paper Contribution

This paper proposes a two-stage approach which includes Spectral Clustering algorithm to correct the deflection of pressure maps and a decision tree to classify sitting postures to ensure a recognition rate (rather than the low rate caused by a

This work is partially supported by The National Key Research and Development Program of China (2016YFB0502201).

limited number and deflection of sitting postures). Our primary contributions can be summarized as follows.

- We use spectral clustering to divide the human sitting area into two sections to resolve any deflection in the pressure map. We then calculate the rotation angle θ to correct the pressure map to the normal direction to ensure a high recognition rate despite changes in the sitting rotation angle. Spectral clustering, or segmentation-based object categorization, is applied to the image segmentation process. The effect of this algorithm is optimal for sitting-area segmentation and yields useful nonlinear pressure array sensor data with high efficiency.
- We create a decision tree for clustering to classify pressure maps by $\text{dis}(c_1, c_2)$ and divide the space of vector into grids of n lines of n columns for the further classification. Different grids represent different clusters. Using the classifier of k-NN, we define the center of each grid as neighbors to be chosen. At last the pressure maps with feature vectors in the same grid are regard as belonging to the same cluster.
- We use a k-NN voting mechanism which is developed with the case being classified by a majority vote of its neighbors to, achieving 92.2% accuracy of identification. We set the K value to 10. After identifying 10 consecutive pressure maps in the temporal domain, we take the largest number of matching results as the final identification result.

II. SYSTEM DESCRIPTION

A. Hardware System

The hardware system iCushion consists of IMM-00014 series pressure array sensors and a data collector. The pressure array sensors number 2,288 and are placed in 52 rows and 44 columns in a criss-cross configuration, as shown in Fig. 1. The collector creates a 2 Hz data transmission frequency. The pressure data is transmitted to the user's PC via a USB interface.

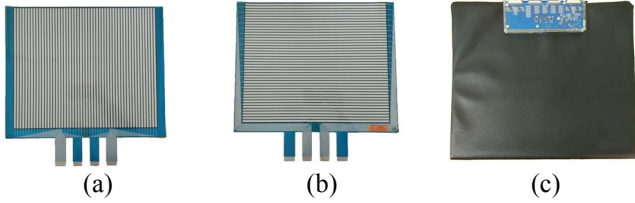


Fig. 1. (a) Front view of pressure array sensors; (b) rear view of pressure array sensors; (c) overall view of iCushion.

TABLE I. SENSOR PARAMETERS

Size of pressure array sensor	52×44
Size of cushion	40.5 cm x 40.5 cm
Cell area	5 mm x 5 mm
Sensor number	2,288
Material	PET
Thickness	$\leq 25 \mu\text{m}$

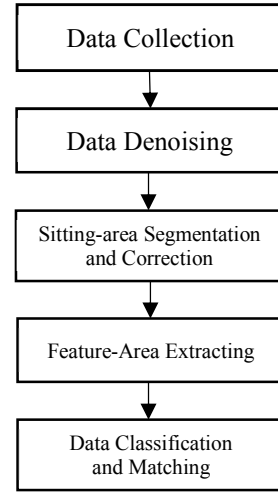


Fig. 2. Algorithm flowchart

B. Algorithm

Our identification algorithm and approach to solving the problem caused by different sitting postures and sitting posture deflection are discussed in this section. As shown in Fig. 2, we first collected the pressure maps of sitting postures. We then ran data denoising to correct sitting posture deflection, feature extraction, and finally data classification and cross-validation to determine how well the data reflects the identity of the sitter.

1) Data pre-processing

a) *Data denoising*: In actual acquisition, due to human or non-human causes, collected maps have a lot of noise as shown in Fig. 3(a). It is necessary to screen for valuable elements. We consider noise to fall into two categories: discontinuous noise and continuous multi-noise, or called "huddled noise". In the former category, elements meeting the following conditions are considered noise:

$$\left\{ w_{ij} \left| \begin{aligned} &(w_{i-1j} = 0 \cap w_{i+1j} = 0 \cap w_{ij} > 0) \\ &\cup (w_{ij-1} = 0 \cap w_{ij+1} = 0 \cap w_{ij} > 0) \end{aligned} \right. \right\} \quad (1)$$

where w_{ij} is the value of the i^{th} row and j^{th} column in the matrix.

In the latter category, we connect each valued element (the value is greater than zero) to their neighbors which are also valued to form a graph $G = (V, E)$. So the nodes of the graph are all valued elements. Then we retain maximal connected subgraphs only the elements of which can reach a certain amount, which we set to 300 in the experiment reported here. The denoised pressure map is shown in Fig. 3(b).

The nodes in G are as follow:

$$\{v | \text{the value of } v > 0\} \quad (2)$$

The edges in G are as follow:

$$\{(u, v) | u \text{ and } v \text{ are adjacent}\} \quad (3)$$

Then we reserve the maximal connected subgraphs $G' = (V', E')$ we want as follow, while the values of elements corresponding to the nodes of other maximal connected subgraphs are set to 0:

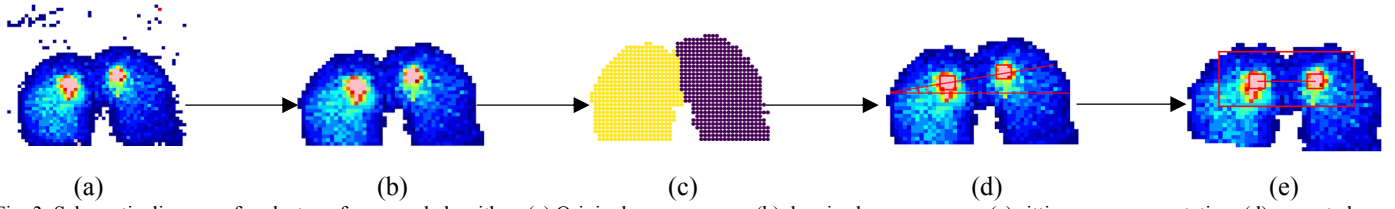


Fig. 3. Schematic diagram of each step of proposed algorithm. (a) Original pressure map; (b) denoised pressure map; (c) sitting-area segmentation; (d) corrected pressure map deflection; (e) feature extraction.

$$\{G' = (V', E') | |V'| \geq \text{miniAmount}\} \quad (4)$$

G' is one of the maximal connected subgraphs of G

b) Sitting-area segmentation: In order to distinguish each half of the sitting area, next we have tried to apply several clustering methods including K-means, Density-based spatial clustering of applications with noise (DBSCAN), and Spectral Clustering for the segmentation of sitting-area pressure maps. The results showed that Spectral clustering method was the most suitable method for this problem. Spectral clustering, also known as segmentation-based object categorization, involving placing objects into clusters based on the eigenvectors and eigenvalues of an associated matrix. Our results are shown in Fig. 3(c).

The target classifies the original data, a $m \times n$ -dimension vector $\{x_1, x_2, x_3, \dots, x_{m \times n}\}$, into two categories where $m \times n$ is the scale of the pressure array sensors. First, we calculate the similarity between each element in the vector to get the similarity matrix $W = \{w_{ij} | 1 \leq i \leq N, 1 \leq j \leq N\}$ as follows:

$$w_{ij} = e^{-\frac{\|x_i - x_j\|^2}{2\sigma^2}} \quad (5)$$

We consider a normalized diagonal matrix D , which is the sum of all the elements in a row of the similarity matrix, to make sure no single element is excluded easily:

$$D(i, i) = \sum_{j=1}^N x_{ij} \quad (6)$$

The normalized Laplacian matrix L is calculated as follows:

$$L = D^{-\frac{1}{2}} W D^{-\frac{1}{2}} \quad (7)$$

The feature-vectors of L are calculated and the vectors with the largest K eigenvalues are placed by columns into a matrix X :

$$X = [v_1, v_2, \dots, v_K] \quad (8)$$

v_1, v_2, \dots, v_K are the vectors with the largest K eigenvalues.

Finally, the matrix X is normalized according to the formula (6) to form the matrix Z , and use the matrix Z to K-means clustering.

c) Correction of pressure map deflection: The actual seated direction of a person is extremely unlikely to match the expected direction, so we must rotate the pressure map to meet our needs. As shown in Fig. 3(d), we identified the ischium areas in both segmented areas defined above which has the highest total pressure value and denoted them D_1, D_2 . We then calculated and corrected the pressure maps with deflected angle θ by connecting the centers of D_1 and D_2 which named c_1 and c_2 . The formula for θ angle correction is as follows:

$$\begin{cases} x' = (x - x_0) \cos \theta + (y - y_0)(-\sin \theta) + x_0 \\ y' = (x - x_0) \sin \theta + (y - y_0) \cos \theta + y_0 \end{cases} \quad (9)$$

where (x, y) are the coordinates corrected before, (x', y') are the corrected coordinates, and (x_0, y_0) is center of the pressure map.

2) Feature extraction

a) Extract feature area: We observed in our experiment that the edge elements of the seating area pressure map fluctuate over a wide range, while the elements surrounding ischium area are relatively stable. Therefore, we regard the rectangular area surrounding the ischial bones as the feature area. To continue, we focused solely on the feature area to improve the accuracy and efficiency of identification.

We first calculated the distance between a pair of ischia as $\text{dis}(c_1, c_2) = \sqrt{(x_{c_1} - x_{c_2})^2 + (y_{c_1} - y_{c_2})^2}$, extracting a rectangular area centered on both ischial areas and with width W of $\text{dis}(c_1, c_2) + a$ and height H of b as the feature area M for subsequent steps in the identification process. The relatively stable area in the “back-leaning” posture is the coccyx, so in this sitting posture, we only extracted a small rectangular area surrounding the coccyx as the feature area. When the distance between the ischial area was less than d , the pressure map was regarded as the result of the back-leaning posture, and only the rectangular area with width W of f and height H of g was extracted. To unify the algorithm flowchart, we set “ $\text{dis}(c_1, c_2)$ ” of this pressure map as d . We set a as 15, b as 15, and d as 10 in the experiment, as shown in Fig. 3(e).

b) Data classification: Different individuals have different pressure features corresponding to their sitting areas, and different pressure features across their own different sitting postures. In order to improve the matching reliability and reduce the quantity of matching times for the sake of efficiency, we only match maps in the same cluster. We find in our experiment that the distance between both ischia we measured is invariable in the same posture but not always in different postures. And the variance in vectors around the ischium which take more forces will be larger. So the distance between both ischia and the variance in vectors around both ischia are extracted as features ($\text{dis}(c_1, c_2), \sigma_L, \sigma_R$) for clustering for their stability in a specific posture.

- Distance between both ischia $\text{dis}(c_1, c_2)$

$$\text{dis}(c_1, c_2) = \text{Max} \left(\sqrt{(x_{c_1} - x_{c_2})^2 + (y_{c_1} - y_{c_2})^2}, 10 \right) \quad (10)$$

- Variance in vectors of left and right bisection in feature area M

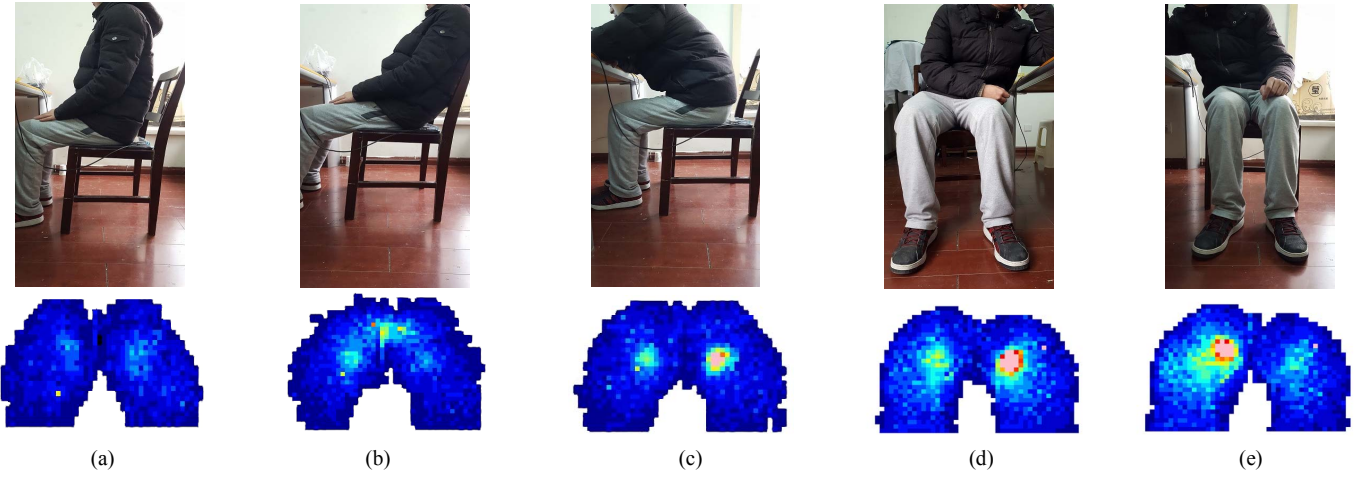


Fig. 4. Five sample sitting postures (a) sitting straight; (b) back-leaning; (c) bending; (d) right-leaning; (e) left-leaning

$$\overline{M}_L = \frac{\sum_{i=0}^{\frac{W}{2}} \sum_{j=0}^H w_{ij}}{\frac{W}{2} * H} \quad (11)$$

$$\overline{M}_R = \frac{\sum_{i=\frac{W}{2}+1}^W \sum_{j=0}^H w_{ij}}{\frac{W}{2} * H} \quad (12)$$

$$\sigma_L = \frac{\sum_{i=0}^{\frac{W}{2}} \sum_{j=0}^H (w_{ij} - \overline{M}_L)^2}{\frac{W}{2} * H} \quad (13)$$

$$\sigma_R = \frac{\sum_{i=\frac{W}{2}+1}^W \sum_{j=0}^H (w_{ij} - \overline{M}_R)^2}{\frac{W}{2} * H} \quad (14)$$

Where \overline{M}_L is the mean value in the vectors in left bisection of M ; \overline{M}_R is the mean value in the vectors in right bisection of M ; σ_L is the variance in the vectors in left bisection of M ; σ_R is the variance in the vectors in right bisection of M . Then we combined σ_L and σ_R into coordinates as a feature vector (σ_L, σ_R) .

As shown in Fig. 5, we create a decision tree for clustering with the first step being to classify pressure maps by $dis(c_1, c_2)$. Then the space of vector (σ_L, σ_R) is divided into grids of n lines of n columns for the further classification with the maximal x-axis of grids being $max(\sigma_L)$ and the maximal y-axis of that being $max(\sigma_R)$. Different grids representing different clusters, we marked each grid (i, j) for grid of i^{th} line and j^{th} column. Using the classifier of k-NN, we define the center of each grid as neighbors to be chosen. The feature vectors (σ_L, σ_R) are placed in the corresponding grids we constructed above, and sample maps with feature vectors in the same grid are regard as belonging to the same cluster.

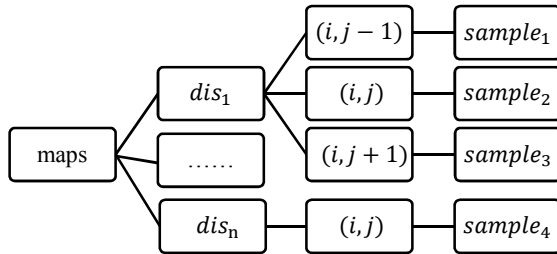


Fig. 5. Decision tree for clustering

3) Feature matching

After we carried out data screening and sample identification, we computed the Euclidean distance with all the sample maps in the corresponding cluster. The test pressure map was successfully matched to sample map k when k met the following condition (though the system did not accept the identity corresponding to the sample map):

$$\begin{cases} Eu_dis_{kT} = \sqrt{\sum_{i=0}^H \sum_{j=0}^W (S_k[i, j] - t[i, j])^2} \leq Th, (k \leq n) \\ Eu_dis_{kT} = \min(\{Eu_dis_i | 1 \leq i \leq n\}) \end{cases} \quad (15)$$

where S is the sequence of the corresponding cluster sample maps, n is the number of sequence samples, T is the pressure map to be matched, Eu_dis_{kt} is the Euclidean distance between T and S_k , and Th is the threshold we set.

4) Voting mechanism in temporal domain

We extracted features in the temporal domain for enhanced accuracy and robustness by using k-NN algorithm. In every k consecutive match, we accept one identity for these test maps, with the case being assigned to the class most common amongst its k nearest neighbors measured by a temporal-distance function. If the quantity of chosen neighbor is lesser than $\frac{y}{2}$, the test map was rejected for identification in any case.

III. EXPERIMENT AND RESULT ANALYSIS

Three participants assisted us in evaluating the proposed iCushion system. Their demographic information is provided in Table II. The participants wore the same clothing throughout the experiment to prevent any extraneous effect on the results. The experiment was run in separate data collection and result analysis phases.

TABLE II. INFORMATION OF PATICIPANTS

Participant	Sex	Age	Height	Weight
A	Male	20	180 cm	90 kg
B	Male	22	175 cm	58 kg
C	Male	22	178 cm	60 kg

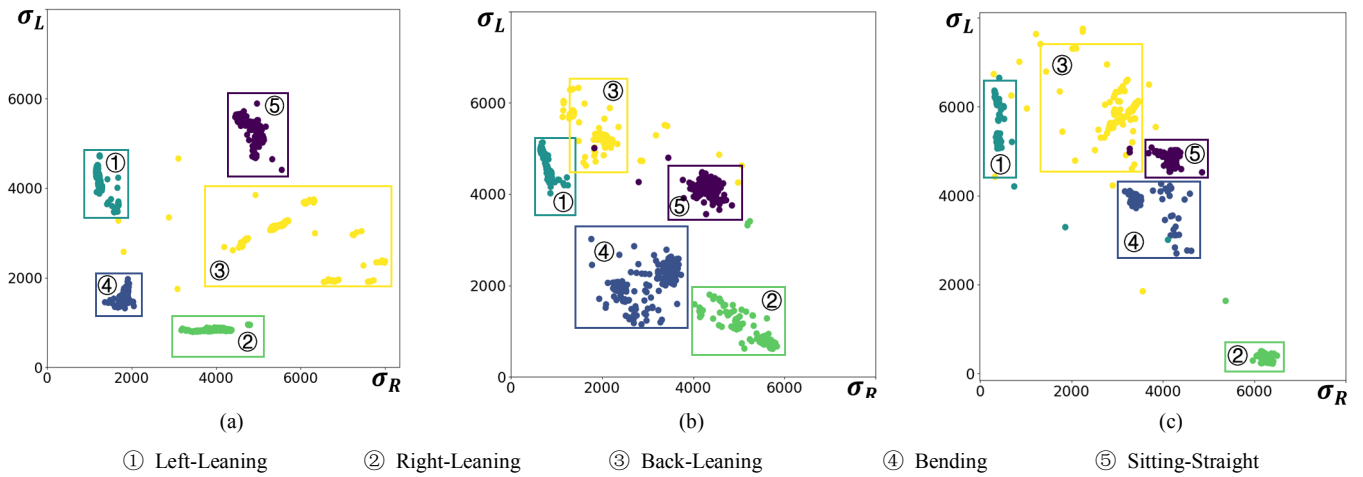


Fig. 6. Variance distribution of 5 sample sitting postures proves different sitting postures have different ischial variances. In fact, we identify people by more sitting postures in experiment 2) (a) Participant A; (b) Participant B; (c) Participant C

A. Data Collection

Experiment 1) We placed iCushion on an office chair with a smooth surface. We collected pressure maps from three participants using five different postures: sitting straight, back-leaning, bending, left-leaning, and right-leaning, as shown in Fig. 4. We collected 200 pressure maps for each sitting posture of each participant.

Experiment 2) We collected the sitting-area pressure maps of each participant about four hours of continuous, normal working, resting, and eating. We collected a total in excess of 100,000 pressure maps. In the process of collecting data for Participant A, for example, our program automatically stored the experimental data in a hierarchical form of “ischial distance-variances coordinates”.

B. Results Analysis

Experiment 1) proves that we can distinguish different sitting postures via ischial spacing and variances. Fig. 6 shows the relationship between sitting postures and variances. When one person sits differently, the corresponding variances are different; when individuals have the same sitting posture, the variances corresponding to each person also differ. For example, as shown in Fig. 6(a), when Participant A sits in a straight posture versus a bending posture, the variance distribution is different and regular. As shown in Fig. 6(b), Participants A and B have different variance distribution when using the same

sitting posture. To this effect, it is feasible to classify sitting postures using variance distributions and then to identify individual sitters.

In *Experiment 2)*, we performed a 10-fold cross-validation on 24,000 maps for each participant on continuous and non-intrusive identification. And we have divided 900 grids with n set 30 in *data classification* step which represented 900 clusters we have clustered. The results are shown in Fig. 7.

We tried Th in Eq. (14) valued from 600 to 1,500 and matched the maps between test datasets and sample datasets. As shown in Fig. 7., when k valued 10 in temporal domain step, we calculated identification rates, FRR, and FAR for all the participants. And we get EER when Th valued 1400, for its value is 3.7%. At this Th value, identification rate achieved 92.2%, which we assert is fully sufficient for identification in any scenario reasonably similar to our experiments.

IV. CONCLUSION

This paper presented a novel authentication system based on pressure array sensors. At its core, our algorithm 1) can identify people continuously and non-intrusively, 2) can distinguish different sitting postures used by the same individual, and 3) can resolve the pressure map deflection problem. We implemented this system on PC, but it can be easily ported to other embedded systems to be widely applied in scenarios such as personal vehicles and offices. We found that our system has high identification accuracy even when users change their postures frequently. In the future, we plan to introduce dynamic information to further enhance the proposed system.

REFERENCES

- [1] Ribeiro, B., HugoAlmeida, RuiFerreira, AdelaideMartins, LeonardoQuaresma, ClaudiaVieira, Pedro, Optimization of sitting posture classification based on user identification. 2015. 1-7.
- [2] Abowd, R.O.A.J.O.D., The Smart Floor: A Mechanism for Natural User Identification and Tracking. 2009.
- [3] Zhou, B., et al., Measuring muscle activities during gym exercises with textile pressure mapping sensors. Pervasive and Mobile Computing, 2017. 38: p. 331-345.

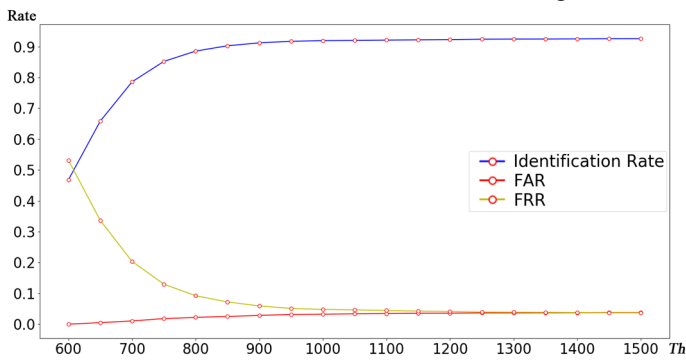


Fig. 7. Result in different thresholds

- [4] Chica, M., et al., Real-time recognition of patient intentions from sequences of pressure maps using artificial neural networks. *Comput Biol Med*, 2012. 42(4): p. 364-75.
- [5] Sundholm, M., et al., Smart-mat, in *Proceedings of the 2014 ACM International Joint Conference on Pervasive and Ubiquitous Computing - UbiComp '14 Adjunct*. 2014. p. 373-382.
- [6] Liang, G., et al., Cushionware, in *Proceedings of the extended abstracts of the 32nd annual ACM conference on Human factors in computing systems - CHI EA '14*. 2014. p. 591-594.
- [7] Pataky, T., Todd C.Mu, TingtingBosch, KerstinRosenbaum, DieterGoulermas, John Y., Gait recognition: highly unique dynamic plantar pressure patterns among 104 individuals. *Vol. 69*. 2012. 790-801.
- [8] Takeda, T., et al., Biometrics Personal Identification by Wearable Pressure Sensor, in *2012 Fifth International Conference on Emerging Trends in Engineering and Technology*. 2012. p. 120-123.
- [9] Zhou, B., et al., The carpet knows: Identifying people in a smart environment from a single step. 2017. 527-533.
- [10] Ferro, M., et al., A Sensing Seat for Human Authentication. *IEEE Transactions on Information Forensics and Security*, 2009. 4(3): p. 451-459.
- [11] Ferscha, A.R., Supporting Implicit Human-to-Vehicle Interaction: Driver Identification from Sitting Postures. 2010.
- [12] Yamada, M.K., K.Kudo, M.Nonaka, H.Toyama, J., Soft authentication and behavior analysis using a chair with sensors attached: hipprint authentication. *Vol. 3*. 2009. 251-261.